Journal of Environmental Chemical Engineering 6 (2018) 2724–2732

Contents lists available at ScienceDirect

Journal of Environmental Chemical Engineering

journal homepage: www.elsevier.com/locate/jece

Efficient photocatalytic removal of RhB, MO and MB dyes by optimized Ni/NiO/TiO_2 composite thin films under solar light irradiation

Qi Zhu, Na Liu, Nan Zhang, Yiying Song, Mishma Silvia Stanislaus, Chenyu Zhao, Yingnan Yang*

Graduate School of Life and Environmental Sciences, University of Tsukuba, 1-1-1 Tennoudai, Tsukuba, Ibaraki, 305-8577, Japan

ARTICLE INFO

Keywords:
Ni/NiO/TiO_2 composite photocatalyst
Solar-light-driven
Dye decomposition
Photocatalytic mechanism
Selective degradation

ABSTRACT

In this study, Ni/NiO/TiO_2 composite powder and thin films were successfully prepared via sol-gel method. The results indicated that Ni/NiO/TiO_2 composite with 2.5% Ni/Ti molar ratio, and the thin film calcined under 400 °C for 2 h with 3 coating layers, demonstrated the highest efficiency for Rhodamine B (RhB) degradation. Over 99.9% of RhB was photocatalytically degraded by Ni/NiO/TiO_2 thin film under 60 min of simulated solar light irradiation, whereas merely 61.9% by pure TiO_2 film. This remarkable ability is caused by suitable amount of Ni and NiO dopant (2.5%), which made the composite present a smaller crystallite size (5.16 nm), bigger specific surface area (154.72 m^2/g), lower band gap energy (2.78 eV) and recombination rate of electron-hole pairs. Additionally, the photocatalytic activity did not exhibit significant loss even after repeated use of ten cycles, suggesting the high stability of the Ni/NiO/TiO_2 thin film. The degradation test of Ni/NiO/TiO_2 thin film for different dyes (Methyl blue, Methyl orange and Rhodamine B) revealed that the photocatalyst has remarkable activity on dye degradation. Moreover, the radical trapping experiments demonstrated that the major active species including $O_2^{\cdot -}$ and ·OH played important roles in the photocatalytic process. The proposed photocatalytic mechanism showed that Ni and NiO could reduce the recombination of photo-generated electron-hole pairs and decrease the band gap energy of composite, resulting in enhanced photocatalytic ability and enlarged solar spectral response range.

1. Introduction

The development of urbanization and industrialization has led to the increased deterioration of water quality, with the shortage of clean water resource highlighted worldwide [1]. The most tough and pervasive problem in wastewater is organic dyes, which arise from textile, printing and food industries [2,3]. Usually, the traditional methods such as adsorption, chlorination and flocculation cannot degrade the dyes completely, and may even generate some toxic intermediates, leading to secondary pollution [4–6]. In view of this, more effective and sustainable methods are needed to degrade those recalcitrant organic pollutants in wastewater effectively.

Basically, semiconductor photocatalysis has been recognized as a very attractive technology for wastewater decontamination. Of the various kinds of photocatalyst, TiO_2 powder photocatalytic treatment has been regarded as the most promising method for degrading dyes in wastewater due to its relatively strong photocatalytic activity, non-toxicity and low cost [7–10]. Nevertheless, there are still some drawbacks limiting its application. For example, the large band gap of TiO_2 (3.2 eV) limits the utilization of solar spectrum, especially in the visible region [11,12]. More importantly, the high recombination rate of photo-generated electron-hole pairs may reduce the reaction efficiency [13–15]. The difficulty of a post-treatment separation stage may affect the application of TiO_2 nanoparticle photocatalyst in the real water environment [16,17].

To improve the practical photocatalytic performance, effort has been doubled to modify TiO_2 by combining with noble metals, such as Ag, Pt and Au [18–21]. Nevertheless, these noble metals are expensive for practical application. Therefore, Ni is deemed to be an appropriate modification material [22]. Compared with other metals, Ni with a lower cost and enhancement of photocatalytic activity under visible light is considered as a solution for inhibiting the recombination of photo-generated electron-hole pairs after combined with TiO_2 [23]. Wang and others [24] reported that after adding 1% of nickel, the activity of TiO_2 for dye degradation can be highly improved. However, these works are just simply discussed the effect of Ni dopant on photocatalytic activity, and there is few research focusing on the optimization of different synthesis conditions (such as the optimum doping amount of Ni, calcination temperature, calcination time or the final state of Ni dopant) and their interaction effect on the properties of

* Corresponding author.
E-mail address: yo.innan.fu@u.tsukuba.ac.jp (Y. Yang).

https://doi.org/10.1016/j.jece.2018.04.017
Received 28 November 2017; Received in revised form 6 April 2018; Accepted 7 April 2018
Available online 09 April 2018

photocatalyst, including crystallite size, band gap energy and specific surface area.

On the other hand, to solve post separation problem in large-scale application of photocatalyst powder, many attempts have been made to immobilize TiO_2 on supports, such as stainless steel, silica, zeolites, activated carbon, for the practical application of TiO_2 photocatalytic technology [25–28]. Given that the inherent light-tight property of these materials may reduce the light absorption in a photocatalytic reactor, transparent glass tube with high transmittance could be a more appropriate support with optimum light harvesting efficiency. Until now, there has been no report about the Ni/NiO/TiO_2 thin films coated on glass tubes. Therefore, it remains a great challenge to find out a low cost, strong oxidizing capability and high stability Ni-doped TiO_2 photocatalyst and coat it on a transparent support as a thin film to overcome the aforementioned problems.

The purpose of this research was to develop a solar-light-driven Ni/NiO/TiO_2 thin film coated on glass tubes for treatment of dyes. The influence of Ni/Ti ratio on composite powder and the optimization of Ni/NiO/TiO_2 thin film by calcination temperature, time and number of coating layers were investigated. The mechanism of dyes purification was also explored by free radical scavenger test. This study would provide a novel viewpoint of developing solar-driven-photocatalyst for low cost dye degradation treatment.

2. Experimental

2.1. Materials

Tetrabutyl titanate ($Ti(OC_4H_9)_4$), ethanol, HNO_3 and $Ni(NO_3)_2$ were utilized as TiO_2 source, solvent, dispersing agent and dopant, respectively. Rhodamine B (RhB), methyl blue (MB) and methyl orange (MO) were used as model organic dyes to evaluate the photocatalytic efficiency, and the structure of dyes are shown in Fig. 1. Benzoquinone, ethylenediaminetetraacetate (EDTA) and *tert*-Butanol (tBuOH) were employed as free radical scavengers. All the reagents were of analytical grade and used without any further purification and purchased from Wako Pure Chemical Industries, Ltd, Japan.

Simulated solar light (XC-100, SERIC., Ltd, Japan) was taken as the irradiation source. Distilled water was used throughout this study.

2.2. Preparation of Ni/NiO/TiO_2 composite photocatalyst powder and thin film

2.2.1. Ni/NiO/TiO_2 composite photocatalyst powder

Samples of Ni/NiO/TiO_2 composite photocatalyst powder was synthesized by sol-gel method. For a typical procedure, 6 mL tetrabutyl titanate was dissolved in 46 mL ethanol. Then, certain amount of Ni $(NO_3)_2$ was dissolved in 11 mL of 1 mol/L HNO_3 solution and added into the above transparent solution drop by drop. A transparent solution was obtained when the two solutions were mixed together by magnetic stirring at room temperature. After 8 h, the transparent sol was obtained, and then was dried at 105 °C for 24 h. The subsequent photocatalyst powder was collected after 2-h calcination under 400 °C in a muffle furnace. Based on the molar ratio of Ni/Ti in composites controlled by amounts of $Ni(NO_3)_2$ and tetrabutyl titanate in raw material, the final products were denoted as 0%, 1.5%, 2.5%, 3.0% and 4.5% Ni/NiO/TiO_2 composite, respectively. Pure TiO_2 was also synthesized under the same condition as control.

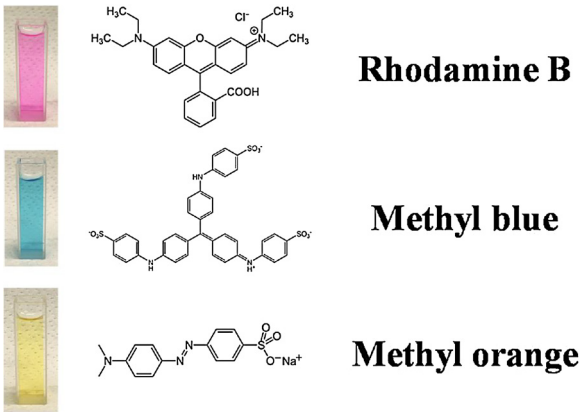

Fig. 1. The structure of Rhodamine B (RhB), Methyl blue (MB) and Methyl orange (MO). (For interpretation of the references to colour in this figure legend, the reader is referred to the web version of this article.)

2.2.2. Ni/NiO/TiO_2 composite thin film on glass tube

To synthesize Ni/NiO/TiO_2 thin film, glass tubes (length: 15 cm, φ: 8 mm, Φ: 10 mm) were employed as thin film carriers. Prior to coating, the entire interface of glass tubes was thoroughly washed with 75% ethanol via ultrasonic method, followed by drying. Then, as prepared sol (Ni/Ti molar ratio: 2.5%) was coated on the inner surface of glass tubes. After coating, the tubes were dried at 105 °C for 24 h and calcined in a muffle furnace at different temperature ranging from 350 °C to 550 °C for varying time from 0.5 to 2.5 h in a muffle furnace. To prepare 1, 2, 3 and 4-layer films, the process of coating and drying were repeated certain times. Finally, the Ni/NiO/TiO_2 composite thin film coated tubes were obtained and stored in a desiccator.

2.3. Analytical techniques

The Scanning Electron Microscope and Energy-dispersive X-ray spectroscopy (FE-SEM(S-4800) + EDS) was employed to investigate the morphology and element ratio of composite powder. X-ray diffraction (XRD) patterns of powder and thin films were characterized by using a Rigaku Altima III Rint-2000 X-ray diffractometer equipped with Cu Kα radiation (λ = 1.54178 Å). The photoluminescence (PL) spectra with an excitation wavelength of 325 nm were acquired with a JASCO FP8500 fluorescence spectrophotometer. UV–vis diffuse reflectance spectra of different samples were recorded in the range of 200–450 nm on a Shimadzu UV-3100PC Scan UV-vis-NIR spectrometer. The specific surface area of the composite photocatalysts was observed by Brunauer-Emmett-Teller (BET) specific surface analysis device (Coulter SA-3100, US).

2.4. Photocatalytic performance evaluation

The photocatalytic performance of as-prepared Ni/NiO/TiO_2 composite powder and thin films were evaluated by RhB, MO and MB degradation. The schematic diagram is showed in Fig. 2. For photocatalyst powder, 0.05 g of photocatalysts (with different molar ratio of Ni/Ti) was dispersed into 50 mL of 2 mg/L aqueous solution of dyes and irradiated under simulated solar light lamp with light intensity of 510 W/m^2. For Ni/NiO/TiO_2 thin film, firstly, the thin film coated tubes were filled up with 3.5 mL of 2 mg/L aqueous solution of dyes. Then, the tubes were fastened on shaker and irradiated under the same light condition with powder degradation test. Samples from the dye solutions was collected at time intervals of 30 min, and analyzed to evaluate the concentration of RhB, MO and MB by a Shimadzu UV-1600 spectrophotometer at λ = 554, 464 and 664 nm, respectively [29,30]. The photocatalytic degradation efficiency was calculated according to Eq. (1):

$$R = \frac{C_0 - C_t}{C_0} \times 100\% \quad (1)$$

where R is the degradation rate (%), C_0 is the initial concentration of reactant (mg/L) and C_t is the reactant concentration after t minutes of irradiation (mg/L).

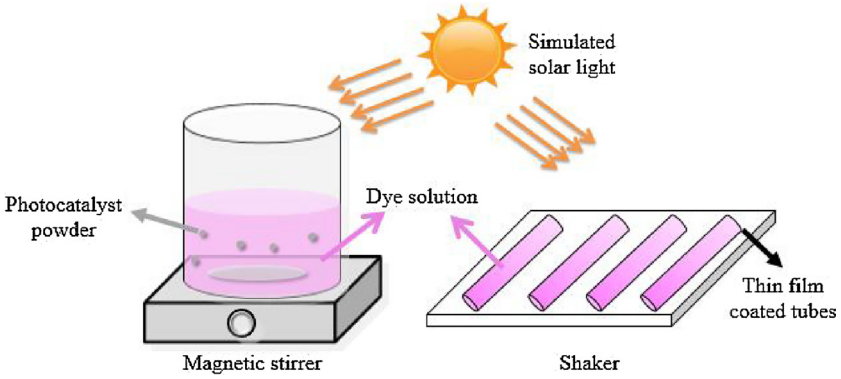

Fig. 2. Schematic diagram of dye degradation experiment by photocatalyst powder and thin film.

2.5. Radical trapping experiment

To investigate the major active species during the photocatalytic degradation process by Ni/NiO/TiO_2 composite film, radical trapping experiments were conducted. The scavengers used in this study were benzoquinone (for $O_2^{\cdot -}$), ethylenediaminetetraacetate (EDTA) (for h^+) and tBuOH (for ·OH). Prior to experiments, 1 mM scavenger was added into RhB solution, following by dark condition to reach the adsorption-desorption equilibrium between the photocatalyst and the dye. After irradiation by simulated solar light, the solution was collected at given time intervals, and the concentration of RhB was measured.

3. Results and discussion

3.1. Optimization of the synthesis of Ni/NiO/TiO_2 composite photocatalyst powder

The composite photocatalyst powder was optimized by adjusting Ni/Ti molar ratio, and the results are displayed in Fig. 3. The results showed that photocatalytic activities were significantly influenced by Ni/Ti molar ratio. The RhB degradation efficiency of Ni/NiO/TiO_2 composite increased from 40% to 91% when Ni/Ti molar ratio increased from 0 to 2.5%. Further increase in the molar ratio from 2.5% to 4.5% led to a decline by 49% in the degradation efficiency. More specifically, the photocatalytic performance of Ni/NiO/TiO_2 catalysts was optimized when the ratio of Ni/Ti equaled 2.5%. This is because a suitable amount of Ni and NiO dopant can act as a bridge to transfer the photo-generated electron-hole pairs to the different part of photocatalyst. Consequently, the recombination of photo-generated electron-hole pairs could be inhibited. Moreover, Hsu et al. reported that, when

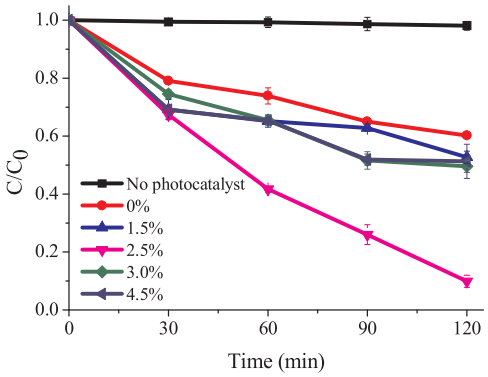

Fig. 3. Degradation rate of RhB by Ni/NiO/TiO_2 powder at different ratios of Ni/Ti under simulated solar light (RhB concentration: 2 mg/L, light intensity: 510 W/m^2). Error bars represents standard deviations from replicate experiments (n = 3).

the amount of dopant was higher than optimal value, the particle size of composite would increase, leading to the decrease in photocatalytic performance [31]. Therefore, when the ratio of Ni/Ti was increased beyond 2.5%, the efficiency of composite photocatalyst decreased.

EDS was employed to investigate the element distribution of the as-prepared Ni/NiO/TiO_2 composite powder with different Ni/Ti ratio. In Table 1, it was detected that the Ni element appeared in all the Ni-doped photocatalyst and the amount increased with the increasing of initial Ni/Ti ratio. This suggest that the Ni dopant has been combined with TiO_2.

To examine the structure and composition of the as-prepared photocatalysts, XRD patterns of 0%, 1.5%, 2.5%, 3.0% and 4.5% powders were analyzed. As shown in Fig. 4, the XRD patterns of all the samples could be well indexed to the anatase phase of TiO_2 (JCPDS 21–1272), where the diffraction peaks at 2θ = 25.0°, 37.6°, 48.0°, 54.9°, 62.3°, 68.5°, 75.0° and 82.7° contributing to (101), (004), (200), (211), (204), (301), (215) and (224) planes, respectively. It has been reported that anatase has a higher photocatalytic oxidation and reduction activity than that of rutile [32,33]. Meanwhile, the peak of metallic Ni (JCPDS file no.01-071-3762) was observed at 2.5%, 3.0% and 4.5% samples, which proved the existence of Ni in the composite. In Fig. 4, the peaks of NiO (110) and NiO (220) at 37.1° and 62.7° were combined with anatase phase of TiO_2 (Fig. 4(a)), and the small peak at 44.8° belonged to Ni° (111) (Fig. 4(b)). Also, it can be found that the intensity of anatase phase peaks increases once the Ni ratio was promoted from 0 to 2.5%, resulting in the increase of photocatalytic performance (Fig. 4(a)). In addition, the crystal size of samples was calculated by Scherrer equation and showed in Table 2. Comparing with other samples, 2.5% sample showed the smallest crystal size (Table 2). Normally, smaller crystal size indicates better crystal structure and energy transformation ability, resulting in higher photocatalytic activity [21]. To be more exact, the present results suggested that doping of Ni and NiO could improve the structure and ability of original TiO_2 photocatalyst, and the composition of Ni-doped material is Ni/NiO/TiO_2.

Ni dopant did not only affect the crystal structure and size of composite, but also influence the specific surface area. According to the BET result (Table 2), when TiO_2 was doped by Ni, the specific surface area of powder would be greatly improved. The specific surface area of 1.5% (145.09 m^2/g), 2.5% (154.72 m^2/g), 3.0% (148.27 m^2/g) and 4.5% (145.87 m^2/g) are much bigger than 0% (20.49 m^2/g), as calculated by N_2 adsorption-desorption isotherm curves in Fig. S1. Large

Table 1
Element distribution of different photocatalysts (Atomic%).

	TiO_2 (0%)	1.5%	2.5%	3.0%	4.5%
O	71.3	69.6	70.9	69.3	68.4
Ti	28.7	30.3	28.7	30.1	30.6
Ni	0	0.1	0.4	0.6	1.0

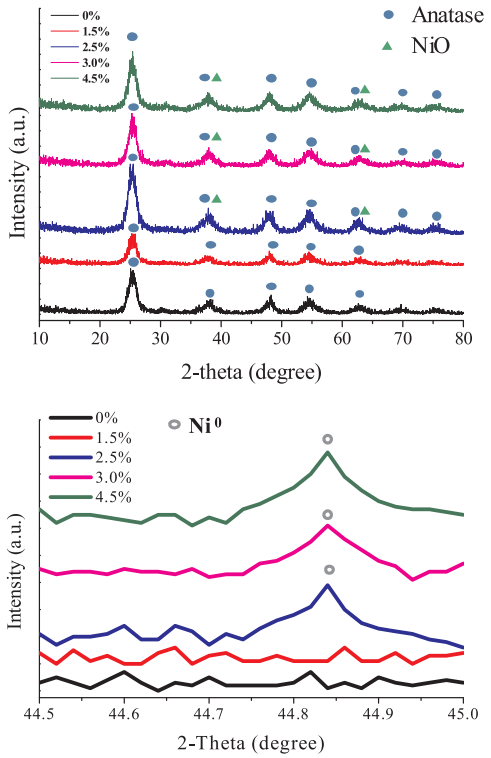

Fig. 4. (a) Full spectrum and (b) Ni^0 peak XRD spectra of TiO_2 and Ni/NiO/TiO_2 powder with different Ni/Ti ratio.

Table 2
Crystallite size and specific surface area of TiO_2 and Ni/NiO/TiO_2 composite with different Ni/Ti ratio.

	TiO_2 (0%)	1.5%	2.5%	3.0%	4.5%
Crystallite size (nm)	5.36	5.55	5.16	5.38	5.39
Specific surface area (m^2/g)	20.49	145.09	154.72	148.27	145.87

specific surface area presents more reaction site on the surface of photocatalyst powder and higher absorption ability [8]. Low specific surface area of 0% sample demonstrated that they could be hard to

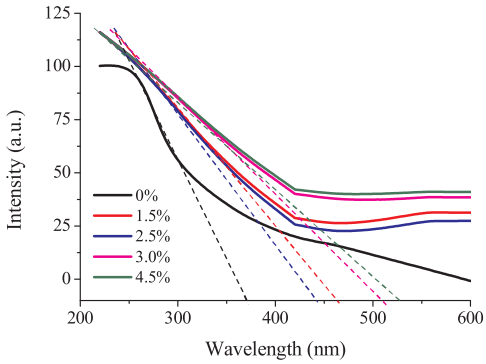

Fig. 6. UV–vis absorption spectra of TiO_2 and Ni/NiO/TiO_2 powder with different Ni/Ti ratio.

absorb enough dye or water for reaction. Also, for 2.5% sample with biggest specific surface area, according to XRD and SEM data, it showed the smallest crystal and particle size (Table 2 and Fig. 5). Normally, smaller crystal and particle size indicates better crystal structure, energy transformation ability and more reaction site, resulting in higher photocatalytic activity [22]. Doping of small amount of Ni and NiO could prevent the growth of the TiO_2 lattice, leading to the increase of specific surface area of the photocatalyst [23,31]. Thus, the photocatalytic performance of Ni/NiO/TiO_2 catalysts could be improved by the Ni and NiO dopants.

The UV–vis absorption spectrum analysis was performed to determine the optical property of the synthesized samples as exhibited in Fig. 6. All the Ni/NiO/TiO_2 composite revealed a stronger light absorption in the wavelength range of 400–600 nm, which belong to the visible light area, compared with pure TiO_2. Based from the UV–vis spectra of the as-prepared samples, the band gap energy of photocatalysts were also calculated [10] (Table 3) using following Eq. (2):

$$Eg = \frac{h\upsilon}{\lambda} \tag{2}$$

Where *Eg* is the band gap energy (eV), h is Planck constant, υ is light speed and λ is the wavelength (nm). The gap energy of 1.5%, 2.5%, 3.0% and 4.5% samples were estimated to be 2.67, 2.78, 2.40 and 2.36 eV respectively, which is much smaller than that of pure TiO_2 (0%, 3.18 eV). These results indicated that the band gap decreased after doping with Ni and NiO. This may account for higher photoactivity of

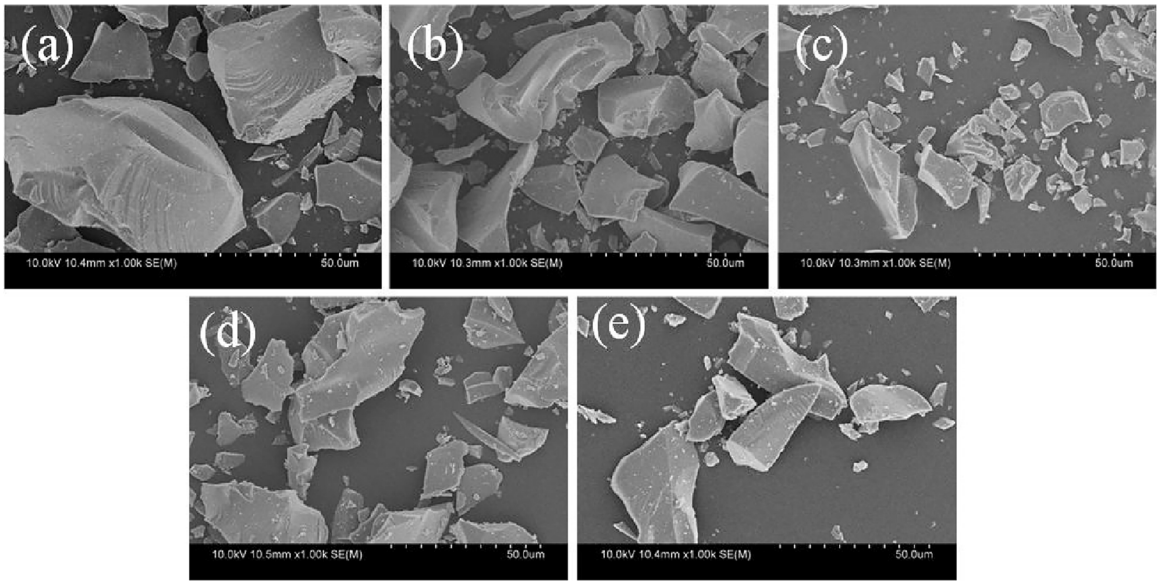

Fig. 5. SEM images of composite powders with different Ni/Ti ratio: (a) 0%, (b) 1.5%, (c) 2.5%, (d) 3.0% and (e) 4.5% (Magnification: 1kx).

Table 3
Band gap energy of TiO_2 and Ni/NiO/TiO_2 composite with different Ni/Ti ratio.

	TiO_2 (0%)	1.5%	2.5%	3.0%	4.5%
Band gap energy (eV)	3.18	2.67	2.78	2.40	2.36

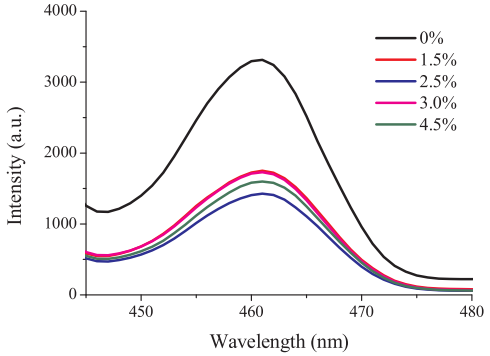

Fig. 7. The PL spectra of TiO_2 and Ni/NiO/TiO_2 powder with different Ni/Ti ratio.

Ni/NiO/TiO_2 composite under the irradiation of simulated solar light.

The morphologies of the 0%, 1.5%, 2.5%, 3.0% and 4.5% Ni/NiO/TiO_2 composite photocatalysts were observed using SEM (Fig. 5). In comparison with TiO_2 (0%) sample, there were many nanoparticles loaded on the surface of the 1.5%, 2.5%, 3.0% and 4.5% Ni/NiO/TiO_2 composite photocatalyst. And comparing with other samples, 2.5% Ni/NiO/TiO_2 photocatalyst sample showed the smallest particle size, which could be contribute to its smallest specific surface area.

Photoluminescence spectroscopy (PL) with broad emission peaks in the region of 445–480 nm was conducted at room temperature to investigate the electron-hole separation of the as-prepared photocatalysts. The PL results were presented in Fig. 7 The emission peak located at 468 nm is attributed to band edge free excitons [13]. It can be easily concluded from Fig. 7 that the sequence of the PL intensities is 2.5% < 4.5% < 3.0% < 1.5% < 0%. Lower fluorescence emission intensity implies lower electron-hole recombination rate and higher photocatalytic activity [12]. With the presence of Ni^0 [23,32] and NiO [33,35], the generated electron can be transfer to the different part of composite, and the electron-hole recombination rate can be highly inhibited. Hence, 2.5% Ni/NiO/TiO_2 catalyst possesses improved photocatalytic activity compared to pure TiO_2 and other photocatalyst with different Ni/Ti ratio.

These results indicated 2.5% as the optimum molar ratio of Ni/Ti for the Ni/NiO/TiO_2 composite photocatalyst with high ability under solar light irradiation, and the photocatalyst with optimum molar ratio was used in the following by experiments.

3.2. Optimization of the synthesis of Ni/NiO/TiO_2 composite photocatalyst thin film

As Ni/NiO/TiO_2 composite powder showed a strong photocatalytic activity after optimization, in order to develop highly efficient photocatalytic film, the effects of calcination temperature, calcination time and coating layers on Ni/NiO/TiO_2 composite films were systematically investigated through photocatalytic degradation of RhB under simulated solar light, and the results are shown in Fig. 8.

Firstly, Ni/NiO/TiO_2 composite films were prepared under calcination varying from 350 °C to 550 °C for 2 h, respectively. It can be found from Fig. 8(a) that the photocatalytic activity of composite film was significantly influenced by calcination temperature. The RhB degradation efficiency of Ni/NiO/TiO_2 composite film increased from 93.9% to 99.9% with calcination temperature increased from 350 °C to 400 °C. Then it largely decreased to 84.7% with temperature further

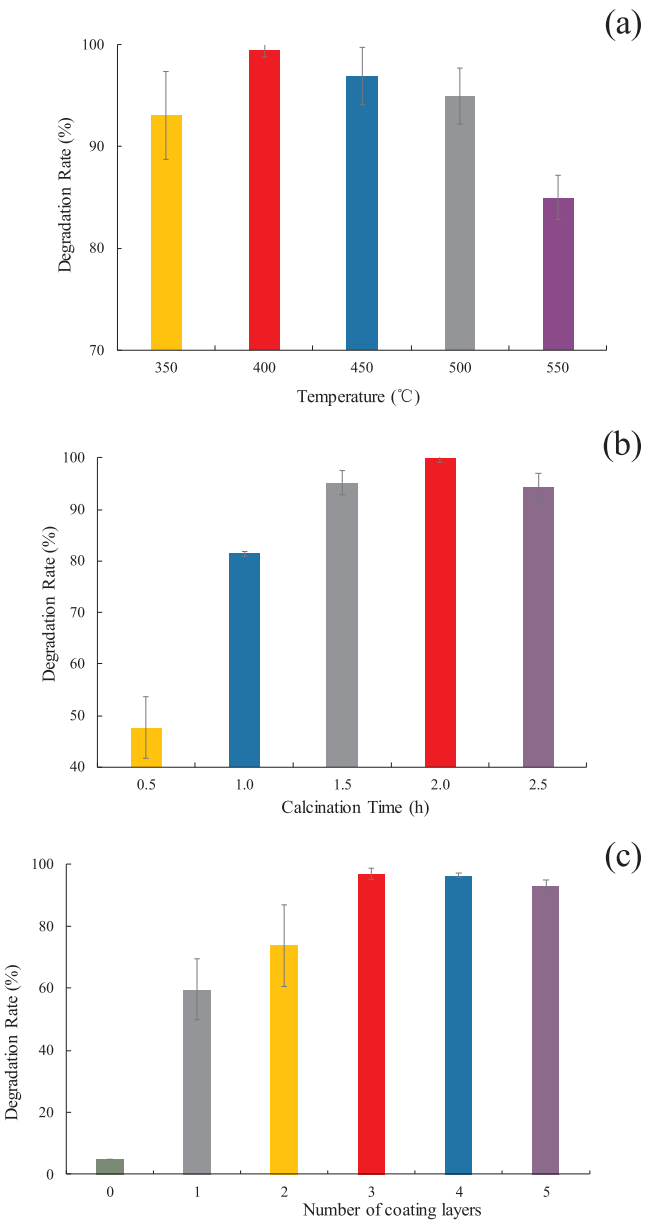

Fig. 8. Effect of (a) calcination temperature, (b) calcination time and (c) number of layers of 2.5% Ni/NiO/TiO_2 thin film on photocatalytic degradation of RhB under simulated solar light (RhB concentration: 2 mg/L, light intensity: 510 W/m^2, reaction time: 1 h). Error bars represents standard deviations from replicate experiments (n = 3).

increased to 550 °C. Long et al. and Ren et al. have reported that the crystallinity of TiO_2 could be influenced by calcination temperature, and the crystallinity of TiO_2 is related to the electrons transport [34,35], which further affect the photocatalytic activity. Chi et al. has reported that the over-calcining temperature may cause serious decomposition of the photocatalyst structure [36], and this might be the reason of low activity of Ni/NiO/TiO_2 composite film prepared at 550 °C. Hence, the optimal temperature for preparing Ni/NiO/TiO_2 composite film is 400 °C.

Calcination time is also an important factor affecting the photocatalytic performance of as-prepared Ni/NiO/TiO_2 films. The effect of calcination time under the optimum temperature 400 °C is presented in Fig. 8(b). When Ni/NiO/TiO_2 films was heat-treated at 400 °C, the photocatalytic activity tends to rise with calcination time, reaching the maximum at the heat treatment time of 2 h, and then descended by further increasing time to 2.5 h. Thus, the optimal calcination time for

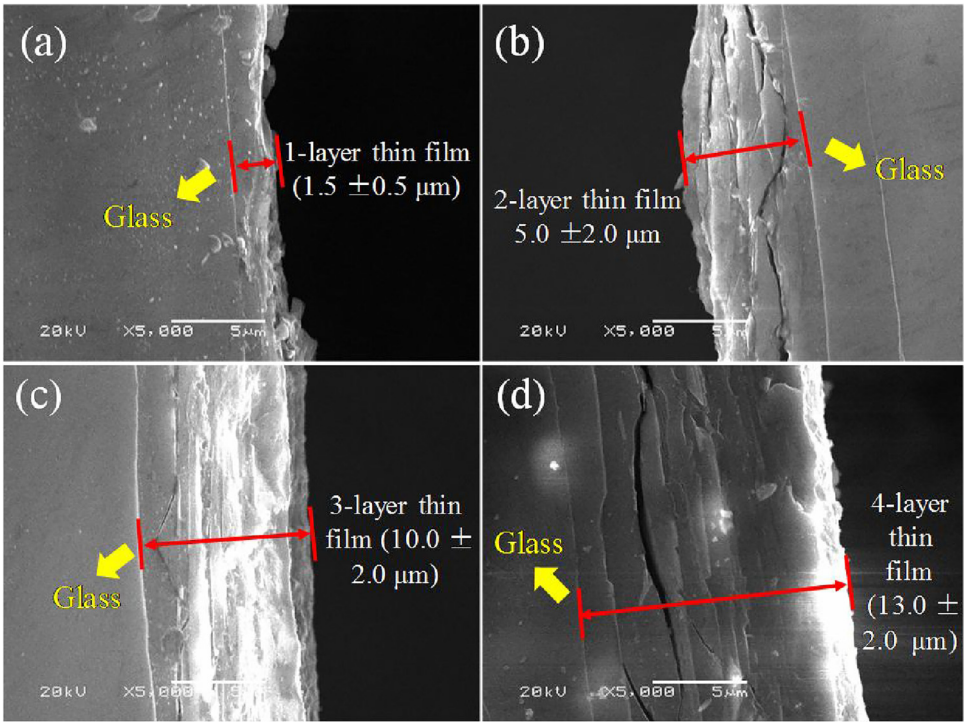

Fig. 9. SEM images of thin film samples with different layers: (a) 1-layer, (b) 2-layer, (c) 3-layer and (d) 4-layer (Magnification: 5kx).

this composite thin film was 2 h. Basically, photocatalytic performance of TiO_2 depends upon whether the electron-hole pairs could be separated efficiently [37,38]. With the optimum calcination time, the suitable structure of Ni/NiO/TiO_2 film could contribute to the reduction of recombination of photogenerated electron-hole pairs [33]. This could be the main reason why Ni/NiO/TiO_2 thin film displayed a maximum photocatalytic activity at 400 °C for 2 h.

Moreover, the photocatalytic performance of Ni/NiO/TiO_2 thin film was affected by the number of coating layers. Fig. 8(c) demonstrates that with increasing number of coating layers, photocatalytic activity showed an upward trend. However, when the number of coating layers further increased to above 3, the degradation rate of RhB fell, suggesting that 3-layer film is the optimum condition. This result may be ascribed to the appropriate thickness of film. And the thickness of 1-layer, 2-layer, 3-layer and 4-layer samples are estimated to be 1.5 ± 0.5, 5.0 ± 2.0, 10.0 ± 2.0 and 13.0 ± 2.0 μm, respectively (Fig. 9). As widely recognized, during photocatalytic reaction, RhB molecules are firstly adsorbed on the solid-liquid intersurface of films, meanwhile the photocatalyst film irradiated under solar light could generate reactive radicals, so the RhB molecule could be degraded by photoinduced free radicals [16]. In 1 and 2-layer samples, the thinner film could not provide enough amount of photocatalyst for reaction. Although 4-layer sample with thicker film could provide sufficient sites for adsorbing RhB molecules, thicker film could block the light irradiation for outside, which may account for the fact that 3-layer film with optimum thickness displayed the greatest photodegradation performance.

Based on the above optimum conditions, Ni/NiO/TiO_2 film coated glass tubes calcined under 400 °C for 2 h with 3 layers were prepared, to degrade RhB solution in comparison with pure TiO_2 thin film. Fig. 10 describes that Ni/NiO/TiO_2 film exhibited much higher catalytic activity than pure TiO_2 film under the irradiation of simulated solar light. Almost 99.9% of RhB solution could be degraded in 1 h by Ni/NiO/TiO_2 film, while the degradation rate of TiO_2 was only around 61.9%. Obviously, Ni/NiO/TiO_2 film presented a promising prospect due to its remarkable potential of photodegradation for wastewater treatment.

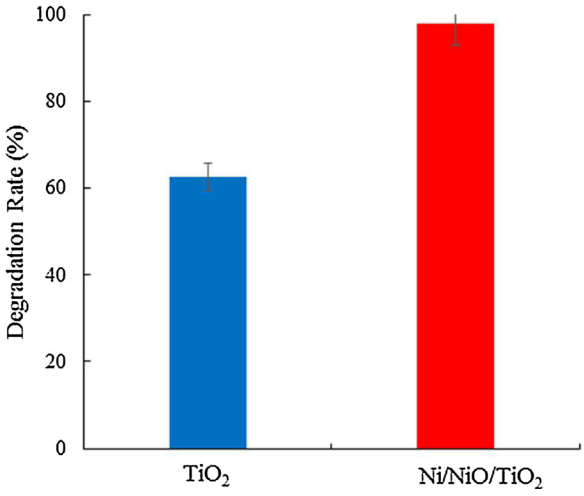

Fig. 10. Photocatalytic activity of TiO_2 and Ni/NiO/TiO_2 thin film coated on glass tubes for degradation under simulated solar light (calcination temperature: 400 °C, calcination time: 2 h, coating layers: 3, RhB concentration: 2 mg/L, light intensity: 510 W/m^2, reaction time: 1 h). Error bars represents standard deviations from replicate experiments (n = 3).

3.3. Repeatability experiment

The reusability of catalyst is crucial for practical application. To evaluate the stability and reusability of Ni/NiO/TiO_2 thin film, the repetitive experiments were conducted, and the results are displayed in Fig. 11. In Fig. 11(a), for the first round of test, the degradation rate of RhB was 99.6%, meanwhile the rate for last round was 99.0%. In the total 10 rounds of test, none of the degradation rates was lower than 99.0%, indicating that the photocatalytic activity of Ni/NiO/TiO_2 composite film did not show significant loss. The highly consistent results for 10 rounds of repetitive test exposed the outstanding stability of Ni/NiO/TiO_2 film.

In addition, XRD patterns (Fig. 11 (b)) showed that there was almost

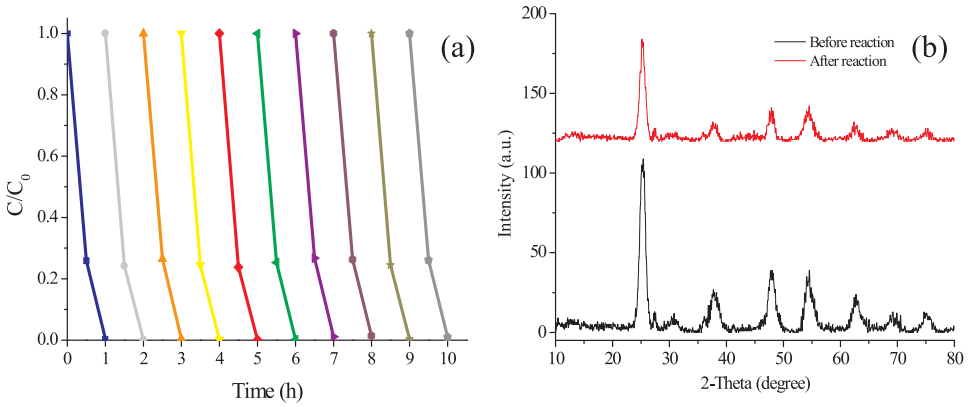

Fig. 11. Repetitive performance of Ni/NiO/TiO_2 thin film coated on glass tubes for RhB degradation under simulated solar light: (a) stability test of RhB degradation (1 h for one cycle); (b) XRD pattern of Ni/NiO/TiO_2 thin film before and after 10 rounds of reaction.

no change between Ni/NiO/TiO_2 composite film before and after ten rounds of photocatalytic reaction. After ten-cycle photocatalytic reaction, Ni/NiO/TiO_2 composite film still exhibited clear and strong peaks at 25.35°, 38.13°, 47.88°, 54.30°, 62.62° and 69.21°, which are ascribed to (101), (004), (200), (105), (204) and (215) planes of anatase phase, respectively. All these results reveal that the Ni/NiO/TiO_2 composite film presents a high photochemical stability and promising use in water environment restoration.

3.4. Comparative photocatalytic degradation of different dyes over pure TiO_2 and Ni/NiO/TiO_2 composite photocatalyst thin film

To determine the feasibility of the Ni/NiO/TiO_2 composite thin film, the comparative photocatalytic activity was further tested through the photodegradation of MB, MO and RhB under simulated solar light with shorter reaction time (30 min). Fig. 12 with the degradation curve of MB, MO and RhB revealed that Ni/NiO/TiO_2 composite thin film has higher activity than pure TiO_2 and selective efficiency on different dyes. For Ni/NiO/TiO_2 composite thin film, about 23.5% of the MO was degraded by the composite thin film, with the degradation rate of RhB and MB reaching 74.4% and 98.0% under simulated solar irradiation, respectively. Under the same conditions, the degradation rate of MO, RhB and MB by pure TiO_2 in 30 min of solar light irradiation, were 7.5%, 45.3% and 56.5%, respectively. It is clear that the Ni/NiO/TiO_2 composite thin film showed higher activity of degradation for all organic dyes than pure TiO_2 and selective efficiency on different dyes.

The main reason for the selective photodegradation efficiency was the photosensitization of dyes. The experiments outlined that dyes could be photosensitized, whereby electron excited from dyes could be ejected to the conduction band (CB) of photocatalyst which further react with oxygen and form superoxide radicals [39–41]. The superoxide radicals in turn are responsible to degrade the dye molecules. The Highest Occupied Molecular Orbital (HOMO) energy gap of RhB, MB and MO are −10.128 eV, −10.494 eV and −5.624 eV, respectively [42]. For RhB and MB, the e^- is easier to be transferred to photocatalyst, which could explain the higher degradation rate of MB and RhB. Although the degradation of MO by Ni/NiO/TiO_2 composite films is lower than MB and RhB, it still much higher than pure TiO_2 thin film. This suggests that the Ni/NiO/TiO_2 composite films has remarkable activity for degradation various kinds of organic dyes.

3.5. Mechanism of photocatalytic activity for Ni/NiO/TiO_2 thin film

To understand the role of active radicals during photocatalytic process, radical trapping experiments were carried out using Ni/NiO/TiO_2 composite films (Fig. 13). According to Fig. 13, compared to the control (without scavengers), RhB degradation efficiency only decreased by 14.9% after 1 h of irradiation by injection of hole (h^+) scavenger (1 mM EDTA). However, photocatalytic efficiency was greatly suppressed by the hydroxyl radical (·OH) scavenger (1 mM tBuOH), with only 47.4% RhB molecules decomposed after 1 h of irradiation. The addition of superoxide anion radical ($O_2\cdot^-$) scavenger (1 mM benzoquinone) resulted in the reduction of photocatalytic efficiency, with 39.8% degradation rate in 1 h. These results suggested that h^+ played less important role on photocatalytic degradation, but $O_2\cdot^-$ and ·OH were the primary active species during photocatalytic process.

Based on the above results, a possible photocatalytic mechanism of

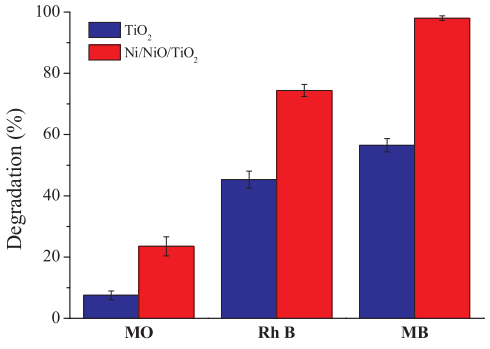

Fig. 12. Photocatalytic degradation of MO, RhB and MB solution by pure TiO_2 and Ni/NiO/TiO_2 thin film under simulated solar light (calcination temperature: 400 °C, calcination time: 2 h, coating layers: 3, dyes concentration: 2 mg/L, reaction time: 30 min, light intensity: 510 W/m^2). Error bars represents standard deviations from replicate experiments (n = 3).

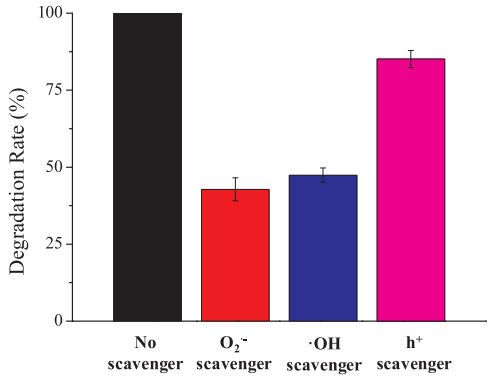

Fig. 13. Photocatalytic degradation of RhB solution by Ni/NiO/TiO_2 in the presence of different scavengers under simulated solar light (calcination temperature: 400 °C, calcination time: 2 h, coating layers: 3, RhB concentration: 2 mg/L, light intensity: 510 W/m^2, reaction time: 1 h). Error bars represents standard deviations from replicate experiments (n = 3).

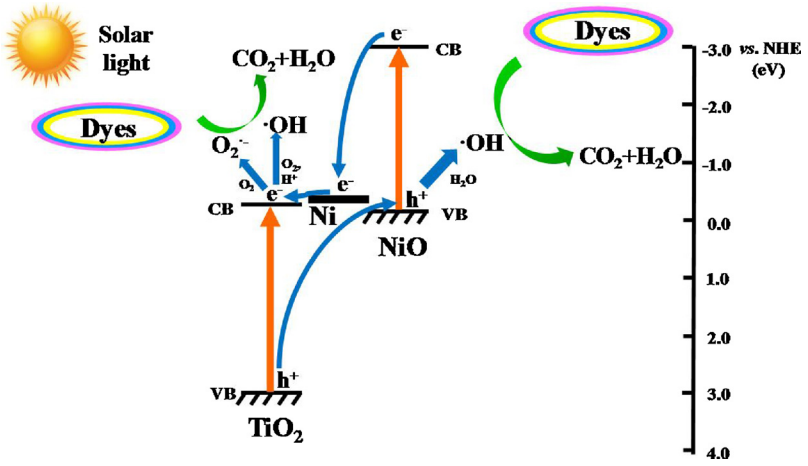

Fig. 14. Photocatalytic mechanism of Ni/NiO/TiO_2 composite film under simulated solar light (↑: charge transfer; ↑: solar light excited e^-; ↑: degradation of dyes).

Ni/NiO/TiO_2 composite film for organic degradation can be illustrated as shown in Fig. 14. The main reactions can be described as below:

$$\text{Photocatalyst} + h\upsilon \rightarrow e_{CB} + h^+_{VB} \quad (3)$$

$$e^-_{CB\text{-}NiO} \rightarrow Ni \rightarrow e^-_{CB\text{-}TiO2} \quad (4)$$

$$h^+_{VB\text{-}TiO2} \rightarrow h^+_{VB\text{-}NiO} \quad (5)$$

$$e^-_{CB\text{-}TiO2} + O_2 \rightarrow O_2^{\cdot -} \quad (6)$$

$$O_2^{\cdot -} + H^+ \rightarrow \cdot HO_2 \quad (7)$$

$$2\cdot HO_2 \rightarrow H_2O_2 \quad (8)$$

$$O_2^{\cdot -} + H_2O_2 \rightarrow \cdot OH + OH^- + O_2 \quad (9)$$

$$h^+_{VB\text{-}NiO} + H_2O/OH^- \rightarrow \cdot OH \quad (10)$$

$$O_2^{\cdot -} + \text{dyes} \rightarrow H_2O + CO_2 \quad (11)$$

$$\cdot OH + \text{dyes} \rightarrow H_2O + CO_2 \quad (12)$$

The transfer of photo-generated electron-hole pairs mainly depends on the value of valence bands (VB) and conduction bands (CB) of TiO_2 (3.0 eV vs. NHE and −0.2 eV vs. NHE) and NiO (0.1 eV vs. NHE and −3.0 eV vs. NHE) as well as Fermi level of Ni (−0.25 eV vs. NHE) [43–46]. After TiO_2 and NiO were excited under simulated solar light irradiation, the photogenerated electrons (e^-) were excited from dyes and VB of TiO_2 and NiO to their CB, and h^+ stayed at VB (Eq. (3)). The excited e^- on CB of NiO could flow to the Fermi level of Ni, and then transferred to the CB of TiO_2 (Eq. (4)), while photo-generated h^+ on the VB of TiO_2 flowed to the VB of NiO (Eq. (5)). Due to the photosensitization of dyes, a number of e^- could be excited to the CB of TiO_2. The transfer of e^- and h^+ could effectively promote charge separation and largely suppress the recombination of photo-generated e^- and h^+ pairs, leading to enhancement of photocatalytic ability. Photo-generated e^- on the CB was mainly absorbed by oxygen (O_2) to generate $O_2\cdot^-$ (Eq. (6)), while the generated $O_2\cdot^-$ and h^+ could create ·OH (Eqs. (7–10)) to react with dye molecules. Finally, organic molecules were completely decomposed during the photocatalytic process by $O_2\cdot^-$ and ·OH radicals (Eqs. (11) and (12)). Although during the degradation of dyes, some intermediates will be generated, including N-de-ethylated and organic acids [47]. However, when the degradation rate of dyes reached to 100%, the residual number of intermediates won't be very high, and the toxicity of the solution would be highly decreased [47,48]. In this way, a variety of dyes can be efficiently purified by low cost solar-light-driven Ni/NiO/TiO_2 composite films.

4. Conclusion

The solar-light-driven Ni/NiO/TiO_2 composite powder and thin films were successfully prepared under optimal conditions by sol-gel method. They exhibited better photocatalytic ability on organic dyes degradation than pure TiO_2 thin films, which benefited from the charge transfer within the composite structure under solar light irradiation. Furthermore, the Ni/NiO/TiO_2 composite films demonstrated consistent stability. The photosensitization of different dyes caused selective activity of Ni/NiO/TiO_2 composite films and the modified photocatalyst thin films showed higher activity on various kinds of organic dyes degradation than pure TiO_2. Due to its high photocatalytic ability and stability, the Ni/NiO/TiO_2 composite films shows a potential for practical application in waste water purification.

Acknowledgements

This work is supported by Scientific Research (B) 15H02859 from Japan Society for the Promotion of Science (JSPS).

Appendix A. Supplementary data

Supplementary data associated with this article can be found, in the online version, at https://doi.org/10.1016/j.jece.2018.04.017.

References

[1] S. Malato, P. Fernández-Ibáñez, M.I. Maldonado, J. Blanco, W. Gernjak, Decontamination and disinfection of water by solar photocatalysis: recent overview and trends, Catal. Today 147 (2009) 1–59.
[2] O. Ozdemir, B. Armagan, M. Turan, M.S. Celik, Comparison of the adsorption characteristics of azo-reactive dyes on mezoporous minerals, Dyes Pigments 62 (2004) 49–60.
[3] S.C.R. Santos, V.J.P. Vilar, R.A.R. Boaventura, Waste metal hydroxide sludge as adsorbent for a reactive dye, J. Hazard. Mater. 153 (2008) 999–1008.
[4] E. Forgacs, T. Cserháti, G. Oros, Removal of synthetic dyes from wastewaters: a review, Environ. Int. 30 (2004) 953–971.
[5] C. Galindo, P. Jacques, A. Kalt, Photooxidation of the phenylazonaphthol AO20 on TiO_2: kinetic and mechanistic investigations, Chemosphere 45 (2001) 997–1005.
[6] K.R. Ramakrishna, T. Viraraghavan, Dye removal using low cost adsorbents, Water. Sci. Technol. 36 (2) (1997) 189–196.
[7] T. Sauer, G.C. Nceto, H.J. Jose, R.F.P.M. Moreira, Kinetics of photocatalytic degradation of reactive dyes in a TiO_2 slurry reactor, J. Photoch. Photobio. A 149 (2002) 147–157.
[8] M. Pelaez, N.T. Nolan, S.C. Pillai, A review on the visible light active titanium dioxide photocatalysts for environmental applications, Appl. Catal. B-Environ. 125 (2012) 331–349.
[9] U.I. Gaya, A.H. Abdullah, Heterogeneous photocatalytic degradation of organic contamination over titanium dioxide: a review of fundamentals, progress and problem, J. Photoch. Photobio. C 9.1 (2008) 1–12.
[10] J.T. Rajesh, K.S. Praveen, G.K. Ramchandra, V.J. Raksh, Photocatalytic degradation of dyes and organic contaminants in water using nanocrystalline anatase and rutile

TiO_2, Sci. Technol. Adv. Mater. 8 (2007) 455–462.
[11] A.K.P.D. Savio, J. Fletcher, K. Smith, R. Iyer, J.M. Bao, F.R. Hernández, Environmentally effective photocatalyst CoO-TiO_2 synthesized by thermal precipitation of Co in amorphous TiO_2, Appl. Catal. B-Environ. 182 (2016) 449–455.
[12] X. Hu, Q. Zhu, X. Wang, N. Kawazoe, Y. Yang, Nonmetal-metal-semiconductor-promoted P/Ag/Ag_2O/Ag_3PO_4/TiO_2 photocatalyst with superior photocatalytic activity and stability, J. Mater. Chem. A 3 (34) (2015) 17858–17865.
[13] Y. Jiaguo, Q. Lifang, J. Mietek, Hydrogen production by photocatalytic water splitting over Pt/TO_2 nansheets with exposed (001) facets, J. Phys. Chem. C 114 (2010) 13118–13125.
[14] Y. Li, S. Sun, M. Ma, Y. Ouyang, W. Yan, Kinetic study and model of the photocatalytic degradation of rhodamine B (RhB) by a TiO_2-coated activated carbon catalyst: effects of iNi-Tial RhB content, light intensity and TiO_2 content in the catalyst, Chem. Eng. J. 142 (2008) 147–155.
[15] Y. Li, X. Zhou, W. Chen, M. Zen, S. Qin, S. Sun, Photodecolorization of rhodamine B on tungsten-doped TiO_2/Activated carbon under visible-light irradiation, J. Hzazrd. Mater. 227 (2012) 25–33.
[16] Q. Zhu, X. Hu, M.S. Stanislaus, N. Zhang, R. Xiao, N. Liu, Y. Yang, A novel P/Ag/Ag_2O/Ag_3PO_4/TiO_2 composite film for water purification and antibacterial application under solar light irradiation, Sci. Total Environ. 577 (2017) 236–244.
[17] D. Li, Q. Zhu, C. Han, Y. Yang, W. Jiang, Z. Zhang, Photocatalytic degradation of recalcitrant organic pollutants in water using a novel cylindrical multi-column photoreactor packed with TiO_2-coated silica gel beads, J. Hazard. Mater. 285 (2015) 398–408.
[18] M. Li, R. Wang, P. Zhong, X. Li, Z. Huang, C. Zhang, Ag-TiO_2-Ag core-shell-satellite nanowires: facile synthesis and enhanced photocatalytic activities, Mater. Lett. 80 (2012) 138–140.
[19] C. Suwanchawalit, S. Wongnawa, P. Sriprang, P. Meanha, Enhancement of the photocatalytic performance of Ag-modified TiO_2 photocatalyst under visible light, Ceram. Int. 38 (2012) 5201–5207.
[20] J. Zhang, M. Zhang, Z. Jin, J. Wang, Z. Zhang, Study of high temperature hydrogen reduced Pt°/TiO_2 by X-ray photoelectron spectroscopy combined with argon ion sputtering-diffusion-encapsulation effect in relation to strong metal-support interaction, Appl. Surf. Sci. 258 (2012) 3991–3999.
[21] H. Wang, J.L. Faria, S. Dong, Y. Chang, Mesoporous Au/TiO_2 composites preparation characterization, and photocatalytic properties, Mater. Sci. Eng. B-Solid 177 (2012) 913–919.
[22] G.G. Nakhate, V.S. Nikam, K.G. Kanade, S. Arbuj, B.B. Kale, J.O. Baeg, Hydrothermally derived nanosized Ni-doped TiO_2: A visible light driven photocatalyst for methylene blue degradation, Mater. Chrm. Phys. 124 (2010) 976–981.
[23] Y. Zhang, Y. Yang, P. Xiao, X. Zhang, L. Lu, L. Li, Preparation of Ni Nanoparticle-TiO_2 nanotube composite by pulse electrodeposition, Mater. Lett. 63 (2009) 2429–2431.
[24] W. Qi, Q. Zenan, C. Jie, R. Baosheng, C. Qifeng, Yanchuan Guo, Xiaofeng Cao, Green synthesis of nickel species in situ modified hollow microsphere TiO_2 with enhanced photocatalytic activity, Appl. Surf. Sci. 364 (2016) 1–8.
[25] J. Shang, W. Li, Y.F. Zhu, Structure and photocatalytic pharacteristics of TiO_2 film photocatalyst coated on stainless steel webnet, J. Mol. Catal. A-Chrm. 202 (2003) 187–195.
[26] M.V.P. Sharma, V.D. Kumari, M. Subrahmanyam, TiO_2 supported over SBA-15: an efficient photocatalyst for the pesticide degradation using solar light, Chemosphere 73 (2008) 1562–1569.
[27] F. Li, S. Sun, Y. Jiang, M. Xia, M. Sun, B. Xue, Photodegradation of an azo dye using immobilized nanoparticles of TiO_2 supported by natural porous mineral, J. Hazard. Mater. 152 (2008) 1037–1044.
[28] M. Baek, J. Yoon, J. Hong, J. Suh, Application of TiO_2-containing mesoporous spherical activated carbon in a fluidized bed photoreactor-adsorption and photocatalytic activity, Appl. Catal. A-Gen. 450 (2013) 222–229.
[29] B. Wang, J. Di, P. Zhang, J. Xia, S. Dai, H. Li, Ionic liquid-induced strategy for porous perovskite-like $PbBiO_2Br$ photocatalysts with enhanced photocatalytic activity and mechanism insight, Appl. Catal. B-Environ. 206 (2017) 127–135.
[30] W. Qin, D. Zhang, D. Zhao, L. Wang, K. Zheng, Near-infrared photocatalysis based on YF_3: Yb^{3+}: Tm^{3+}/TiO_2 core/shell nanoparticles, Chem. Commun. 46 (2010) 2304–2306.
[31] M. Hsu, C. Chang, Ag-doped ZnO nanorods coated metal wire meshes as hierarchical photocatalysts with high visible-light driven photoactivity and photostability, J. Hazard. Mater. 278 (2014) 444–453.
[32] A. Utsunomiya, A. Okemoto, Y. Nishino, K. Kitagawa, H. Kobayashi, K. Taniya, Y. Ichihashi, S.M. Nishiyama, Study of reaction mechanism on ammonia photodecomposition over Ni/TiO_2 photocatalysts, Appl. Catal. B-Environ. 206 (2017) 378–383.
[33] W. Peng, Z. Xu, C. Luo, H. Zhao, Tailor-Made core-Shell CaO/TiO_2/Al_2O_3 architecture as a high-Capacity and long-life CO_2 sorbent, Environ. Sci. Technol. 49 (13) (2015) 8237–8245.
[34] S. Chen, S. Zhang, W. liu, W. Zhao, Preparation and activity evaluation of p-n junction photocatalyst NiO/TiO_2, J. Hazard. Mater. 155 (1) (2008) 320–326.
[35] L. Long, J. Li, L. Wu, X. Li, Enhanced photocatalytic performance of platinized CdS/TiO_2 by optimizing calcination temperature of TiO_2 nanotubes, Mater. Sci. Semicon. Proc. 26 (2014) 107–111.
[36] L. Ren, Y. Zeng, D. Jiang, The improved photocatalytic properties of P-type NiO loaded porous TiO_2 sheets prepared via freeze tape-casting, Solid State Sci. 12 (2010) 138–143.
[37] C. Chi, S. Liau, Y. Lee, The heat annealing effect on the performance of cdS/CdSe-sensitized TiO_2 photoelectrodes in photochemical hydrogen generation, Nanotechnology 2 (2009) 025202.
[38] M. Khan, O. Yang, Photocatalytic water splitting for hydrogen production under visible light on Ir and Co ionized titania nanotube, Catal. Today 146 (2009) 177–182.
[39] Y. Yang, X. Li, J. Chen, L. Wang, Effect of doping mode on the photocatalytic activities of Mo/TiO_2, J. Photoch. Photobio. A 163 (3) (2004) 517–522.
[40] V. Priyanshu, K.S. Sujoy, Facile synthesis of TiO_2–PC composites for enhanced photocatalytic abatement of multiple pollutant dye mixtures: a comprehensive study on the kinetics, mechanism, and effects of environmental factors, Res. Chem. Intermediat. (2017) 1–26, http://dx.doi.org/10.1007/s11164-017-3209-8.
[41] V. Priyanshu, K.S. Sujoy, Degradation kinetics of pollutants present in a simulated wastewater matrix using UV/TiO_2 photocatalysis and its microbiological toxicity assessment, Res. Chem. Intermediat. 43 (11) (2017) 6317–6341.
[42] X. Chang, M. Gondal, A. Al-Saadi, M. Ali, H. Shen, Q. Zhou, J. Zhang, M. Du, Y. Liu, G. Ji, Photodegradation of rhodamine B over unexcited semiconductor compounds of BiOCl and BiOBr, J. Colloid. Interf. SCI 377 (1) (2012) 291–298.
[43] J. Zhao, C. Chen, W. Ma, Photocatalytic degradation of organic pollutants under visible light irradiation, Top. Catal. 35 (3) (2005) 269–278.
[44] A.L. Linsebigler, G. Lu, J.T. Yates, Photocatalysis on TiOn surfaces: principles mechanisms, and selected results, Chem. Rev. 95 (1995) 735–758.
[45] J. Bandara, C. Divarathne, S. Nanayakkara, Fabrication of n-p junction electrodes made of n-type SnO_2 and p-type NiO for control of charge recombination in dye sensitized solar cells, Sol. Energ. Mater. Sol. C 81 (4) (2004) 429–437.
[46] Standard Electrode Potentials, (2018) http://www.physchem.co.za/data/electrode_potentia.htm (Accessed 05 November 17).
[47] H. Zhong, S. Cheng, Y. Shaogui, D. Youchao, H. Huan, W. Zhiliang, Photocatalytic degradation of rhodamine B by Bi_2WO_6 with electron accepting agent under microwave irradiation: mechanism and pathway, J. Hazard. Mater. 162 (2009) 1477–1486.
[48] C. Giuseppe, C.; Luigi A. Francesca, C. Matilde, C. Andrea, V. Francesco, L. Francesco, Photocatalytic degradation of a model textile dye using Carbon-doped titanium dioxide and visible light, J. Water Process. Eng. 20 (2017) 71–77.